JACS
JOURNAL OF THE AMERICAN CHEMICAL SOCIETY
Article
pubs.acs.org/JACS

Conductance of Tailored Molecular Segments: A Rudimentary Assessment by Landauer Formulation

Min-Jie Huang,[§] Liang-Yan Hsu,[§,†] Ming-Dung Fu, Su-Ting Chuang, Fang-Wei Tien, and Chun-hsien Chen*

Department of Chemistry and Center for Emerging Material and Advanced Devices, National Taiwan University, Taipei, Taiwan 10617

Supporting Information

ABSTRACT: One of the strengths of molecular electronics is the synthetic ability of tuning the electric properties by the derivatization and reshaping of the functional moieties. However, after the quantitative measurements of single-molecule resistance became available, it was soon apparent that the assumption of negligible influence of the headgroup−electrode contact on the molecular resistance was oversimplified. Due to the measurement scheme of the metal−-molecule−metal configuration, the contact resistance is always involved in the reported values. Consequently the electrical behavior of the tailored molecular moiety can only be conceptually inferred by the tunneling decay constant (β_n in $R_{measured} = R_{n=0}e^{\beta nN}$, where N is the number of repeated units), available only for compounds with a homologous series. This limitation hampers the exploration of novel structures for molecular devices. Based on the Landauer formula, we propose that the single-molecule resistance of the molecular backbones can be extracted. This simplified evaluation scheme is cross-examined by electrode materials of Au, Pd, and Pt and by anchoring groups of thiol (−SH), nitrile (−CN), and isothiocyanate (−NCS). The resistance values of molecular backbones for polymethylenes (n = 4, 6, 8, and 10) and phenyl (−C_6H_4−) moieties are found independent of the anchoring groups and electrode materials. The finding justifies the proposed approach that the resistance of functional moieties can be quantitatively evaluated from the measured values even for compounds without repeated units.

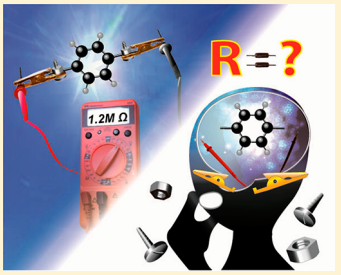

INTRODUCTION

The flourishing development of the quantitative measurements[1−7] for single-molecule resistance accelerates the exploration of electron transport through molecules, once a hypothetical concept proposed by Aviram and Ratner in 1974.[8] The paramount breakthroughs were achieved by the measurement schemes of carbon-based covalently bridged junctions[9,10] and an MMM (metal−molecule−metal) configuration utilizing MCBJ (mechanically controllable break junction)[1,11−15] or SPM (scanning probe microscopy)[2,16−23] which made possible nanometer-spaced molecular junctions between two metallic electrodes. To have the junction accommodate molecules of interest, it is desirable that the molecular terminal groups exhibiting affinity to the electrode materials or with the potential to furnish covalent contacts.[9,10,24−27] It was soon realized that the reported values of single-molecule conductance are strongly dependent on the nature of the molecule−electrode contact, rather than the electric properties of the tailored molecular segment alone. For example, measurements of STM bj (scanning tunneling microscopy break junction) typically find multiple sets of conductance values, ascribed to variations in headgroup−electrode binding geometries.[28−33] Simulation results[34−36] suggest that the binding sites at pyramidal (atop) or pyramidal vacancy (hollow) are preferentially involved in the lower (LC) and higher conductance (HC) sets, respectively. The resistance ratios of LC to HC measured on gold electrodes are ca. 5-, 10-, 10-, and 12-fold for α,ω-alkanes of dithiols,[28,30,37] diisothiocyanates,[30] diamines,[28] and dicarboxylic acids,[28] respectively. The resistance of hexanedithiol (HC) is ca. 10.5 MΩ,[28] significantly smaller than those of its analogues with anchoring groups of diamine (43 MΩ),[28] diisothiocyanate (66 MΩ),[30] and dicarboxylic acid (258 MΩ).[28] On platinum electrodes, hexanedithiol exhibits a resistance of 5.2 MΩ (HC),[38,39] only one-half that on gold electrodes. In addition, for the molecules with the benzene moiety, the resistance values of 1,4-benzenedithiol and 1,4-benzenediamine on gold electrodes are found to be, respectively, 1.2[40] and 2.0 MΩ.[6] These examples show that the contact resistance makes difficult our evaluation of the conductive performance for the molecular backbones. To better correlate the electric behavior with the structural characteristics and thus to facilitate the rational design for future molecular electronics, it would be valuable to have a simple mathematical procedure that places greater emphasis on the conductance of the molecular framework.

Demonstrated herein is that the conductance of the tailored molecular framework can be extracted by utilizing Landauer formulation in the coherent elastic tunneling (superexchange) regime. The equation becomes $G = G_0 T_{contact}(T_{unit})^N$ for $N \geq 1$ (see the Supporting Information), where the conductance (G) is correlated with the conductance quantum ($G_0 = 2e^2/h$ = 77.5

Received: August 27, 2013

   dx.doi.org/10.1021/ja4088538 | J. Am. Chem. Soc. XXXX, XXX, XXX−XXX

μS or 12.9 kΩ) by the transmission probability of the incoming electrons which are scattered by the contact ($T_{contact}$) and N repeated molecular backbone units (T_{unit}). According to the equation, the conductance of the molecular backbone unit, $G_{unit} = T_{unit}G_0$, can be readily obtained because in many cases the contact resistance ($R_{n=0}$) is already available. This approach has not yet been applied to assess the conductance of molecular backbones. For a homologous series of molecules, $R_{n=0}$ can be derived by a linear extrapolation of the resistance values to the intercept against the number of repetitive units, n. Since α,ω-alkanes are commonly studied in the field of single-molecule conductance, they will be the model compounds in this work. To look into the results of this primitive and straightforward approach for G_{unit}, this simple concept is interrogated and cross-examined by the resistance values of polymethylene chains acquired at electrodes of Au, Pd, and Pt. We previously documented the resistance results of alkanedithiols on Au and Pt and those of alkanediisothiocyanates on Au, Pd, and Pt.[38] To expand the database for α,ω-alkanes on these electrode materials, the electrical properties of alkanedinitriles (NC-$(CH_2)_n$CN, n = 2, 4, 6, and 8) are scrutinized and will be reported in the Results. The resistance of the polymethylene chains and a few representative molecular frameworks will then be discussed after the contact resistance is decoupled from those obtained via the MMM configuration.

EXPERIMENTAL SECTION

All chemicals were analytical grade. Alkanedinitriles (NC$(CH_2)_n$CN, n = 2 from Acros, n = 4 from Alfa Aesar, n = 6 and 8 from Sigma-Aldrich) were used as supplied without further purification. STM tips were mechanically cut gold, palladium, or platinum wires (0.25 mm in diameter, 99.95%, Leesan, Tainan, Taiwan). Gold substrates were prepared by thermal evaporation of 100-nm-thick gold on glass slides with a precoated adhesive layer of 10-nm chromium (99.99%, Super Conductor Materials, Suffern, NY). Palladium and platinum substrates were deposited by a 20-W magnetron DC sputtering in Ar plasma (5 mTorr) for 20 min (Co-sputtering System, Kaoduen, Taipei, Taiwan). The glass slides were cleaned by piranha solution composed of a 1:3 (v/v) mixture of 30% H_2O_2 and concentrated H_2SO_4, which *reacts violently with organics and should be handled with great care.*

The experimental procedures and data acquisition for STM break-junction measurements were described in detail elsewhere.[2,20,30] Briefly, the experiments of single-molecule conductance were carried out with a NanoScopeIIIa controller equipped with a current amplifier with a gain of 100 nA/V for the measurements of ethanedinitriles and 10 nA/V for other molecules (Veeco, Santa Barbara, CA). The STM was first operated in the imaging mode with an appropriate tunneling current to survey the tip and substrate conditions. If the acquired images were reasonably stable, indicative of clean substrate and a sharp tip, the working mode was switched to the STS-$I(s)$ mode to obtain curves of current as a function of tip stretching. The measurements were carried out in toluene containing 1−5 mM alkanedinitriles. MMM junctions were created by repeatedly moving the STM tip into and out of contact with the substrate at a rate of 4.2−5.6 nm/s (0.93 Hz). During the process, one or more alkanedinitrile molecules were able to bridge between the tip and the substrate via the cyano anchoring group and complete a molecular junction. The $I(s)$ profiles of current-to-tip stretching were obtained at a fixed tip−substrate E_{bias}, recorded by a NanoScope built-in program, and exported as ASCII files. All traces were analyzed using an automated algorithm to filter out smoothly decayed or noisy curves (see the Supporting Information). The resulting traces exhibited stepwise features in which the conductance values were orders of magnitude smaller than 1 G_0, suggesting the formation of MMM junctions. Each histogram was constructed from more than 1500 traces (out of ca. 8000 curves) and plotted using a logarithmic scale with a linear bin (Origin 8.6, OriginLab). Peak positions and standard deviations were determined using Gaussian fits to the histogram profiles.

Quantum-chemical calculations of the adsorption energy and geometries were performed using the Gaussian 03 program package. The adsorbate structures of butanenitrile on metal surface were optimized based on the density functional theory using Becke's three-parameter exchange functional with the Perdew−Wang91 correlation functional (B3PW91). The 6-31+G(d) basis set was employed to describe nonmetallic atoms. Au, Pd, and Pt atoms were treated by the LANLDZ relativistic effective core potential. The cluster model of a total of 36 atoms was used for the electrode surface, consisting of four-layered (3 × 3) unit cell. The geometry of the adsorption complex was simulated by having the energy of all atoms of butanenitrile relaxed and having the structure of metal clusters fixed based on the experimental lattice constant.[41] The adsorption energy of butanenitrile on the metal surface were described as $E_{ads} = E_{tot} - (E_{surf} + E_{mol})$, where E_{tot}, E_{surf}, and E_{mol} are the total energy of the adsorption complex, the energy of the metal surface, and the energy of the butanenitrile molecule, respectively. The σ and π characters in two-center Mayer bond order were utilized to analyze the headgroup−electrode bond (AOMix).[42,43]

Transmission spectra of alkanedinitriles were obtained by first-principle calculations (Atomistic Toolkit software package, ATK2008) with the combination of DFT treatment in the electronic structure and nonequilibrium Green's function (NEGF) formalism to simulate coherent transport. A double-ζ plus polarization (DZP) basis set was used for all atoms in alkanedinitrile molecules. A single-ζ plus polarization (SZP) basis set was used for metal atoms with a local density approximation in the calculation. The total transmission function $T(E)$ is a sum of transmission probabilities of all channels at energy E under applied bias. The conductance (G) was obtained from the slope in the ohmic region between 0 and 0.2 V.

RESULTS

Single-Molecule Conductance of Alkanedinitriles. The conductance measurements of alkanedinitriles with 2, 4, 6, and 8 methylene units by STM bj method were carried out at molecular junctions of Au, Pd, and Pt electrodes. Figure 1 displays the results of butanedinitrile in a logarithmic scale. The upper panels show typical conductance-distance traces, recorded upon the tip being retracted away from the substrate. Under a fixed E_{bias}, the stepwise fashion of the traces confirms the presence of molecules in the junctions and thus the

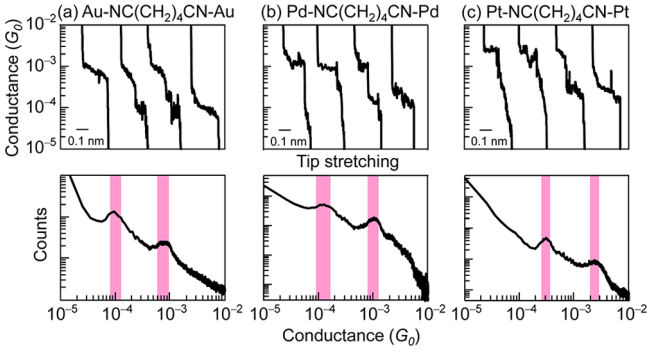

Figure 1. Conductance traces and histograms of NC$(CH_2)_4$CN measured on (a) Au, (b) Pd, and (c) Pt electrodes by STM bj. Top: typical conductance-distance traces obtained by stretching the molecular junctions at a rate of ~5 nm/s. Bottom: log−log conductance histograms constructed from more than 1500 conductance traces. Experiments were carried out in toluene containing 1 mM butanedinitrile. Gaussian fits to the profiles of histograms were used to determine the peak positions and the error bars listed in Table 1. The shades indicate the ranges of standard deviation.

dx.doi.org/10.1021/ja4088538 | J. Am. Chem. Soc. XXXX, XXX, XXX−XXX

Table 1. Single-Molecule Conductance of Alkanedinitriles on Au, Pd, and Pt Electrodes

	Au−NC−$(CH_2)_n$−NC−Au		Pd−NC−$(CH_2)_n$−NC−Pd		Pt−NC−$(CH_2)_n$−NC−Pt	
n	HC[a] ($\times 10^{-4}$ G_0)	LC[a] ($\times 10^{-4}$ G_0)	HC ($\times 10^{-4}$ G_0)	LC ($\times 10^{-4}$ G_0)	HC ($\times 10^{-4}$ G_0)	LC ($\times 10^{-4}$ G_0)
2	59 ± 16	6.8 ± 2.1	73 ± 19	9.1 ± 3.4	166 ± 46	23.7 ± 6.1
4	7.7 ± 1.7	1.0 ± 0.2	10.1 ± 2.1	1.2 ± 0.3	23.9 ± 4.4	3.0 ± 0.6
6	1.1 ± 0.2	0.12 ± 0.03	1.2 ± 0.2	0.14 ± 0.02	2.9 ± 0.6	0.39 ± 0.09
8	0.12 ± 0.02	*b*	0.16 ± 0.03	*b*	0.43 ± 0.09	*b*

[a]HC and LC denote high- and low-conductance sets, respectively. The values of standard deviation are obtained from Gaussian fitting. [b]The LC values of octanedinitrile (n = 8) are unavailable due to the detection limit of the instrument.

Table 2. Summary of β_n, $G_{n=0}$, and Probability for Alkanedinitriles on Au, Pd, and Pt Electrodes

	Au−NC−$(CH_2)_n$−CN−Au		Pd−NC−$(CH_2)_n$−CN−Pd		Pt−NC−$(CH_2)_n$−CN−Pt	
	HC	LC	HC	LC	HC	LC
β_n	1.03 ± 0.02	1.02 ± 0.04	1.03 ± 0.01	1.05 ± 0.02	1.00 ± 0.02	1.026 ± 0.004
β ($Å^{-1}$)[a]	0.83 ± 0.02	0.81 ± 0.03	0.822 ± 0.009	0.84 ± 0.01	0.80 ± 0.01	0.821 ± 0.004
$G_{n=0}$ (G_0)[b]	0.050 ± 0.007	0.0055 ± 0.0009	0.059 ± 0.004	0.0078 ± 0.0007	0.13 ± 0.01	0.0183 ± 0.0004
$R_{n=0}$ (kΩ)[b]	260 ± 37	2328 ± 376	220 ± 14	1643 ± 151	102 ± 9	703 ± 14
probability (%)[c]	55	41	63	33	72	23

[a]β is estimated by employing L values of 0.60, 0.85, 1.10, and 1.35 nm, respectively, for fully extended ethane-, butane-, hexane-, and octanedinitrile. The molecular dimensions were simulated by MM2 (molecular mechanics calculator2) embedded in Chem3D. [b]$R_{n=0}$ and $G_{n=0}$ are, respectively, the contact resistance and contact conductance obtained from the intercepts of Figure 2. $G_0 = 2e^2/h \approx (12.9\ k\Omega)^{-1}$. [c]Frequency of occurrence was reported using the $I(s)$ traces of $NC(CH_2)_4CN$.

formation of MMM structures. Otherwise, the conductance trace decays exponentially with the retracted distance of the tip. The conductance histograms shown in the bottom panels of Figure 1 are prepared from more than 1500 conductance traces in which those exhibiting pure tunneling decay are excluded by an algorithmic program (see the Experimental Section and Figure S1, Supporting Information). The histograms of butanedinitrile reveal features of two conductance sets in which the values of HC (high conductance) sets are about 8-fold those of LC (low conductance) sets acquired at the corresponding electrode material. As mentioned in the Introduction, multiple conductance sets have, in general, been attributed to the difference in their preferential headgroup−electrode contact geometries.[28−30,34]

Conductance histograms of ethane-, hexane-, and octanedinitrile are deposited in the Supporting Information. All histograms exhibit two sets of conductance, except for octanedinitrile whose LC values are expectedly smaller than the detection limit of the instrument. Table 1 summarizes single-molecule conductance of alkanedinitriles. The conductance values of alkanedinitriles on Pd and Pt are 1.3−3.1-fold larger than those on Au. The frequencies of molecule-junction formation for butanedinitrile are about 15% for Au, 18% for Pd, and 23% for Pt, significantly lower than those of 27−42% found for thiol and isothiocyanate headgroups.[30,38] The difference in their probability indicates weaker −CN−electrode adsorption than those of thiol and isothiocyanate (vide infra). The relative occurrence of junction formation between thiol and nitrile headgroups agrees well with the study of diphenylacetylenes on gold electrodes by Wandlowski et al.[44]

Tunneling Decay Constant and Contact Conductance of Alkanedinitriles. The length dependence of the molecular conductance for a homologous series is described by the simple tunneling model[45−47] $G \propto \exp(-\beta_n N)$ or $\exp(-\beta L)$, where N and L are the number of repeated units and the molecular length, respectively. β, the tunneling decay constant, represents the electronic-coupling strength of the molecule along the electron pathway and is obtained from the slope of the least-squares line by plotting the resistance against n. For α,ω-alkanes, two β_n values of ∼1.0[20,24] and ∼0.45[3,19,48] have been reported. The former is ascribed to electron transfer via coherent and nonresonant tunneling (i.e., superexchange) through the alkane framework. A recent study suggested that the latter arises from nonequivalent isomers with gauche structures.[19] In this present study, β_n is found ∼1.0 for both HC and LC sets measured on all electrodes (Table 2), suggesting that the multiple resistance sets are unlikely a result of conformational isomers and hence are attributed to different −CN−electrode binding geometries.

Electrode materials perturb the measured single-molecule conductance via two means:[7] (1) the alignment of the electrode Fermi level (E_{Fermi}) with the frontier molecular orbitals (FMOs, i.e., HOMO/LUMO) and (2) the electronic coupling at the contact between the electrode and the anchoring group.[49−54] To make straightforward the study of the latter, saturated polymethylene chains were employed as the model system by taking advantage of their large HOMO−LUMO gaps.[55,56] The FMOs are far away from the electrode E_{Fermi}, resulting in negligible variation of the tunneling barrier height ($\sim|E_{FMO} - E_{Fermi}|$) between the electrode materials. Tables 1 and 2 manifest how the electrode materials (viz., Au, Pd, and Pt) affect the resistance of alkanedinitriles. The extrapolation of the least-squares fitting to the intercept (Figure 2) confers the contact conductance ($G_{n=0}$). Among the three electrodes, −CN−Pt bears the largest $G_{n=0}$, about 2-fold more conductive than those of −CN−Au and −CN−Pd. The indistinguishable values of β_n support that the difference between their barrier heights is insignificant. The discrepancy in their $G_{n=0}$ is hence ascribed to the electronic coupling strength at the headgroup−electrode contact.

The model molecule is butanenitrile, instead of butanedinitrile, to simplify the simulation of headgroup−electrode interactions. The binding configurations for butanenitrile at atop and hollow sites of the electrode are optimized by allowing butanenitrile to relax freely, while the positions of metal atoms were fixed. The results (Table 3) show the adsorption of −CN

dx.doi.org/10.1021/ja4088538 | J. Am. Chem. Soc. XXXX, XXX, XXX−XXX

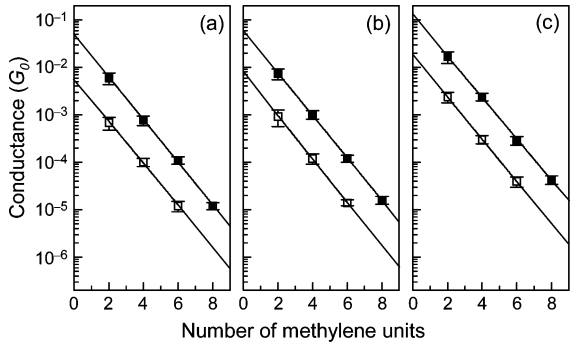

Figure 2. Semilogarithmic plots of single-molecule conductance versus the number of methylene units for (a) Au−NC$(CH_2)_n$CN−Au, (b) Pd−NC$(CH_2)_n$CN−Pd, and (c) Pt−NC$(CH_2)_n$CN−Pt with n = 2, 4, 6, and 8. The slopes and intercepts of the linear fits yield the electronic coupling constant (β_n) and the contact conductance ($G_{n=0}$), respectively, for HC (solid square) and LC (open square) groups.

Table 3. DFT Calculations of Butanenitrile Adsorbed on Au, Pd, and Pt Electrodes

	$CH_3(CH_2)_3$−CN−M				
	adsorption energy (eV)				
electrode material (M)	hollow site	atop site	$E_{hollow} - E_{atop}$	angle (∠CNM)	π:σ characteristics (M−N) (%)
Au	−0.846	−0.649	−0.197	156.75°	12.8:87.2
Pd	−0.995	−0.716	−0.278	179.19°	29.0:71.0
Pt	−1.273	−0.851	−0.422	179.78°	31.9:68.1

on hollow sites is 0.42−0.20 eV/mol more stable than that on atop sites of the corresponding electrode material. Through the cross-examination of the findings in Tables 2 and 3, it is worth noting that the more stable it is for the hollow site over the atop site, the higher is the occurrence probability for the HC events. This trend suggests that the HC and LC traces can be ascribed to the binding configurations of atop-hollow and atop−atop geometries, respectively.[28−30]

Displayed in Figure 3 are optimized structures of butanenitrile adsorbed atop sites of Au, Pd, and Pt electrodes.

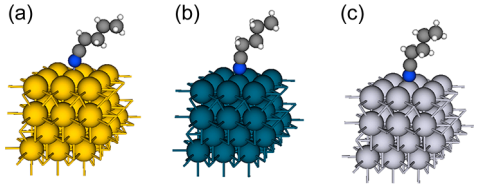

Figure 3. Side views of butanenitrile adsorbed on atop sites of (a) Au, (b) Pd, and (c) Pt. The angles of ∠CNPd and ∠CNPt are linear, consistent with the trend that −CN−Pd and −CN−Pt bear more significant π characters than −CN−Au.

−CN−Au appears bent, yet linear, for −CN−Pd and −CN−Pt, consistent with literature findings[38,49,57] that Au has a significant *s*-orbital contribution while Pd and Pt use more *d*-orbital characters, leading to, respectively, more σ characteristics for the former and more π characteristics for the latter. The occurrence of π character is expected to offer an additional conducting channel,[20,38,49] resulting in conductance superior to those with only one σ channel. To gain quantitative description, simulation results of the relative π-to-σ contribution of headgroup-metal bonds are summarized in Table 3 in which the π character is the smallest at Au and the largest at Pt electrode. Mayer two-center bond order[38] is utilized to quantify the headgroup−electrode contact and yields bond orders of 0.271, 0.387, and 0.594, respectively, for −CN−Au, −CN−Pd, and −CN−Pt (Figure 4). The good correlation of contact

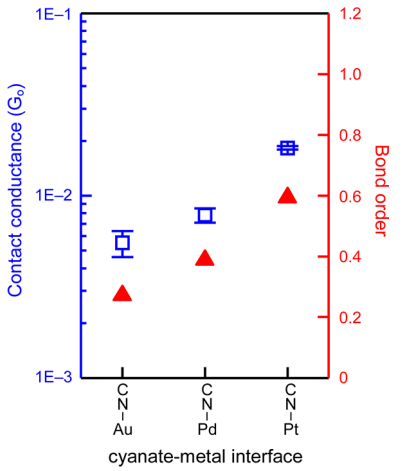

Figure 4. Correlation between contact conductance and Mayer bond order at −CN−electrode contact. Blue squares (left axis): measured $G_{n=0}$. Red triangles (right): bond order.

conductance with the π characters and bond orders manifests the significance of the −CN−electrode electronic coupling on the measured single-molecule conductance.

Transmission Spectra. To look into the conduction features at the contact, the transport calculations for alkanedinitriles are carried out by using the method of NEGF-DFT (nonequilibrium Green's function combined with density functional theory). Figure 5 shows the zero-bias

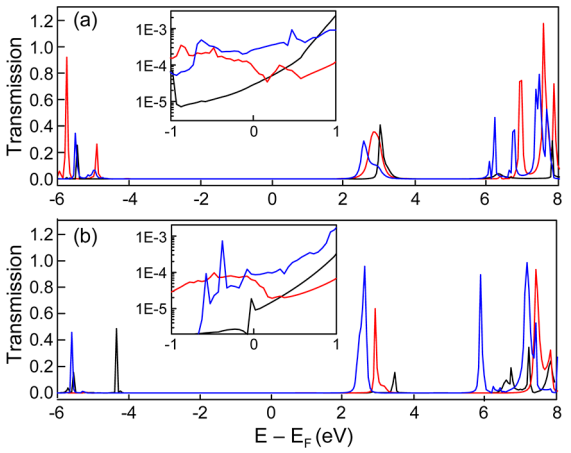

Figure 5. Zero-bias transmission of hexanedinitrile on Au (black), Pd (red), and Pt (blue) for (a) atop−hollow and (b) atop−atop configurations. Displayed in the insets are semilogarithmic plots within ±1 V.

transmission spectra of hexanedinitrile bridging in the atop−hollow and atop−atop configurations. The integration of the transmission ranging from 0 to 0.2 V confers the simulated I−V characteristics. The slope at the ohmic region shows small-bias conductance (Table S1, Supporting Information) with the largest conductance for Pt and the smallest for Au, in agreement with the experimental trend.

dx.doi.org/10.1021/ja4088538 | J. Am. Chem. Soc. XXXX, XXX, XXX−XXX

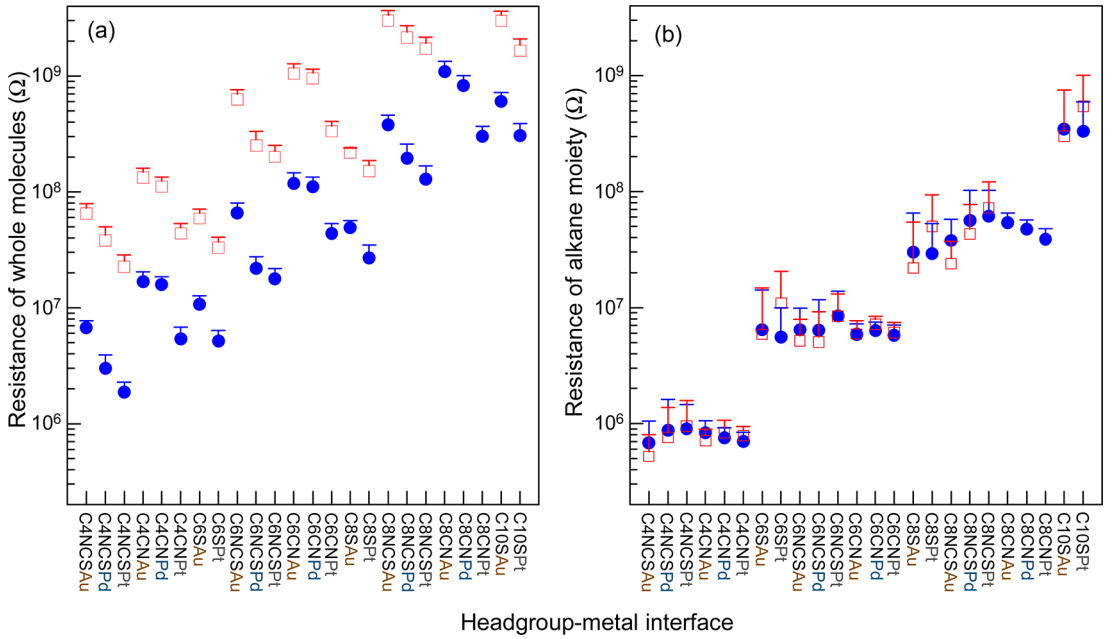

Figure 6. Semilogarithmic plots of (a) experimentally measured single-molecule resistance and (b) estimated resistance of α,ω-alkane backbones. To reduce the complexity of the x-axes, only one side of the headgroup−electrode is labeled. The blue circles and red squares represent HC and LC, respectively. The values in panel a are from literature reports (see Table S2, Supporting Information).[38] To obtain the decoupled results of Panel b, the corresponding $R_{n=0}$ values employed are listed in Table 2 and Table S3 of the Supporting Information.

Given the fact of large HOMO−LUMO gaps for polymethylene chains, no energy level of the molecule is anticipated to contribute resonantly to the transmission around the E_{Fermi} (i.e., $E - E_{\mathrm{Fermi}} = 0$ eV in Figure 5). The magnified insets reveal small transmission features near E_{Fermi} which, based on literature reports,[58−61] are contributed mainly by metal-induced gap states (MIGS), arising from the hybridization of the headgroup with the electrode. As a result, the energy levels of anchoring groups are shifted to the vicinity of E_{Fermi} and appear discrete. The transmission coefficients at the low-bias regime are hence affected by the headgroup−electrode coupling. The stronger the coupling is, more pronouncedly the MIGS broadens and overlaps with the Fermi level of electrodes, leading to a higher transmission around E_{Fermi}. Figure 5 shows that the transmission at E_{Fermi} is larger for Pt than those for Pd and Au. The stronger electronic coupling of −CN group on Pt electrode is consistent with the results of Mayer bond order. Taken together, the difference in their conductance values is ascribed to the headgroup−electrode coupling.

DISCUSSION

Resistance of Molecular Backbone. The conductance of molecular wires is described by the Landauer equation, $G = (2e^2/h)T_{\mathrm{lc}}T_{\mathrm{mol}}T_{\mathrm{rc}}$, where the product of T_{lc} and T_{rc} represents the transmission probability at the left and right contact, respectively, and T_{mol} is the transition probability of an electron from the left (right) contact, passing through the molecule, to the right (left) contact. Arithmetically, with a readily available T_{contact}, the efficiency of electron transmission through the molecular framework unit (T_{unit}) can be conveniently decoupled from G. To interrogate this simple yet unattempted approach, Figure 6 collects resistance values of α,ω-alkanes measured at different headgroup−electrode contacts. Those with the same number of methylene units are arranged together, followed by headgroups and electrode materials. Only one side of the headgroup−electrode pair is labeled in the x-axes to make the abscissae less crowded. Figure 6a shows that the reported values of single-molecule resistance are dependent on molecular chain lengths, anchoring groups, electrode materials, and headgroup−electrode contact geometries, viz., the conductance sets of HC (circles) and LC (squares). After taking T_{contact} away from the MMM scheme, the resistance values of polymethylenes are obtained for C_4, C_6, C_8, and C_{10} (Figure 6b). The striking feature is that the resistance values for the same molecular framework become organized on the same order of magnitude. The independence of anchoring groups and electrode materials demonstrates that it is reasonable to extract the intrinsic resistance of molecular segments by this simple approach.

To further explore the generality of this approach, particularly for molecules with delocalized electrons and for those lack of repeated units, we focus on the decoupled resistance of the $-(p\text{-}C_6H_4)-$ moiety. Benzene receives enormous attention because it has been a model compound for conjugated molecules.[24,63−66] In addition, experimental measurements of homologous series of phenyls (viz., phenyls, biphenyls, and terphenyls) confers accessible contacts of −S−Au,[40,67] $-NH_2-$Au,[6] and covalently bonded $-CH_2-$Au.[25] Hence, the decoupled results mark reference values of $-(p\text{-}C_6H_4)-$ (at ca. 0.09 MΩ) for those lacking available contact resistance. For the latter case, the resistance of $-(p\text{-}C_6H_4)-$ is estimated by utilizing $R_{n=0}$ adopted from α,ω-alkanes with corresponding headgroups. This approach is proposed because Wandlowski and co-workers demonstrated that the contact resistance of thiol-terminated oligo(phenylene-ethylene) derivatives is similar to those acquired from Au−alkanedithiol−Au junctions,[68] indicative of insignificant influence on $R_{n=0}$ by the electronic structure of molecular backbone. Indeed, $R_{n=0}$ for 1,4-phenyls and α,ω-alkanes appears reasonably close with the respective values of −S−Au[38] and $-NH_2-$Au[6,20] being 186 and 130, and 330 and 370 kΩ.

dx.doi.org/10.1021/ja4088538 | J. Am. Chem. Soc. XXXX, XXX, XXX−XXX

Displayed in Figure 7 for 1,4-disubstituted benzenes are literature values bearing the contact resistance (red) and those

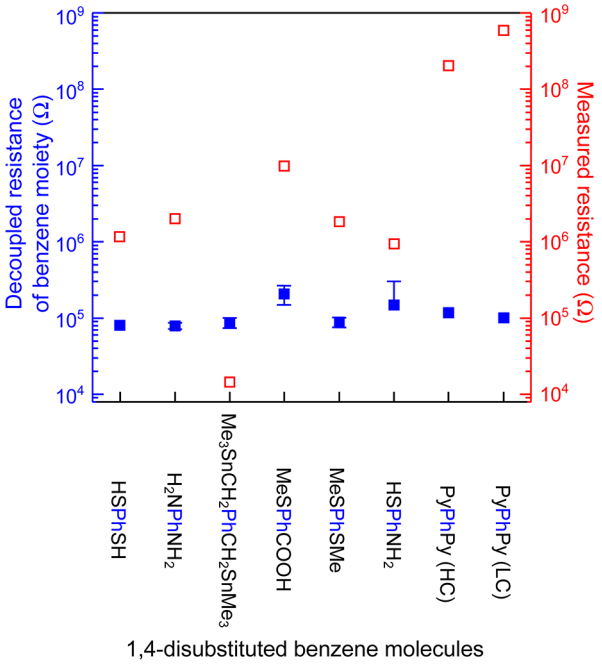

Figure 7. Plot of resistance for benzene moieties prior to (red, open) and after (blue, solid) being decoupled by using $R_{n=0}$ from literature reports (see Table S4, Supporting Information). The span of resistance values of 5 orders of magnitude (0.014−600 MΩ) for the measured MMM junctions is reduced to be less than 1 order of magnitude (80−200 KΩ) for the estimated −(*p*-C_6H_4)− moiety. For the last two examples, −(*p*-C_6H_4)− with pyridyl termini has two conductance sets.[62] Error bars: propagation of the standard deviation of $R_{n=0}$.

of decoupled −(*p*-C_6H_4)− (blue). DFT calculations suggest that there are σ and π channels for electron transport through −(*p*-C_6H_4)−, and the former is more resistive by 1 order of magnitude.[24,25,70] Those in Figure 7 all transport through the π channel. Conducting via the σ channel is suggested for the example of $Me_3SnPhSnMe_3$ which is a precursor and subsequently develops covalent aromatic carbon−gold contacts (Au−C_6H_4−Au).[24] The resistance (2.7 MΩ) of the −(*p*-C_6H_4)− moiety after decoupled ($R_{n=0}$ = 3.1 kΩ or 4.2 G_0) is not displayed in Figure 7 to avoid confusion with those via the π channel. The formation of covalent methylene carbon−gold bonds also takes place for $Me_3SnCH_2PhCH_2SnMe_3$ and results in the contact of Au−CH_2−C_6H_4−CH_2−Au. The pathway of π channel through this MMM junction is suggested by DFT calculations.[25] The decoupled resistance of −(*p*-C_6H_4)− is about the same as those using chemisorbed contacts. Figure 7 shows that the resistance values for −(*p*-C_6H_4)− derived from a wide range of contacts are consistent, demonstrating the satisfactory application of this approach to molecular segments with conjugated moieties and/or without homologous series.

This present work emphasizes on tailored molecular moieties that have no repeated units. For such cases, β_n is unavailable, making difficult the assessment of the electron-transfer efficiency through the designed framework. The decoupling arithmetic demonstrated in Figures 6 and 7 is a simple routine to quantitatively estimate the resistance value essentially for all kinds of molecular backbones. Table 4 shows selected examples of molecules with fascinating moieties. At first glance, the conjugation along the backbone, the measured molecular resistance, and β values are uncorrelated. After decoupling $R_{n=0}$ from the measured MMM resistance, the last column of Table 4 shows that the moiety with a superior conjugation (or with a smaller β) renders a smaller resistance although the length of the segment needs to be taken into consideration. Thus, this approach offers a quick means to comprehend the correlation between the molecular structure and its resistance.

Resistance of Molecular Segments Derived from a Tight-Binding Model along with Landauer Formulation. In an AFM work on monolayer conductance, Frisbie and co-workers[50] found and looked into the independence of the decay parameter (β_n) on the electrode work function and the applied bias voltage. This finding is counterintuitive to what Simmons equation is modeled for electron tunneling across an insulator with a square-shaped energy barrier.[71] Simmons equation concludes that the decay parameter is a function of the barrier height, $\beta = 2(2m\phi/\hbar^2)^{1/2}$, where m, ϕ, and $\hbar$ are effective electron mass, the barrier height, and the reduced Planck constant, respectively. Because the barrier height is associated with both the electrode work function and the applied bias voltage, the above-mentioned independent correlation was unexpected. Thoroughly examined in that study were 18 types of contacts with MMM combinations composed of molecules of alkane monothiols and dithiols, and electrode materials of Au, Ag, and Pt. For those using the same electrode material, the extrapolated $R_{n=0}$ for monothiols was very different from that of dithiols, with the former 1−2 orders of magnitude more resistive than the latter. In addition, the molecular conductance was length-dependent, involving a constant β_n of ∼1.1 per methylene unit (or 0.88 $Å^{-1}$). Hence, to explain why β_n is a constant, transmission theory based on the Landauer equation was utilized to investigate transport probabilities across the molecular junctions ($T(E_{Fermi}) = T_{substrate}\cdot T_{mol}\cdot T_{tip} = T_{contact}\cdot T_{mol}$). Derived from the measured resistance data, the extrapolated $R_{n=0}$, and the estimated number of molecules under the AFM tip (10−100 molecules), the authors showed that T_{mol} can be described by a transmission value of ∼0.33 per carbon−carbon bond (T_{C-C}, $\exp(\beta_n N) = 1/T_{mol} = 1/(T_{C-C})^N$). To validate this T_{C-C} of ∼0.33, resistance values of monothiol and dithiol junctions were predicted by multiplying the T_{C-C} with its corresponding $R_{n=0}$. The comparison was made with experimental results of a total of 54 MMM junctions. The predicted junction resistance was correlated linearly with the measured values, demonstrating that the approach of transmission theory offered a good description for the independence of β_n on the electrode work function and the applied bias voltage.

In the approach of Frisbie and co-workers,[50] T_{mol} is defined by $T_{mol} = |V_{C,C}/(E_C - E_{Fermi})|^{2n}$, the ratio of the overlap energy of neighboring methylene units against the energy difference between the electrode E_{Fermi} and the methylene carbon. Alternatively, elaborated concisely herein is the donor-bridge-acceptor model,[78,79] which describes electron propagation along the molecular wire and correlates well the electron-transporting probability with the corresponding β value of the molecular framework.[63,78] To account for the effect of contacts and to correlate the conductance of the molecular backbone with the experimental values, we start from the Landauer approach $G = G_0 T(E_{Fermi})$ and then reformulate the corresponding molecular Green's function to incorporate the left (l) and right (r) anchor groups, $(\mathbb{G}_{mol})_{l,r}$, for the molecule

dx.doi.org/10.1021/ja4088538 | J. Am. Chem. Soc. XXXX, XXX, XXX−XXX

Table 4. Estimated Resistance of Selected Molecular Segments

molecular structure	single-molecule resistance (MΩ)	β value (Å^{-1})	$R_{n=0}$ (MΩ)	ref no.[a]	molecular backbone	estimated resistance (MΩ)[b,c]
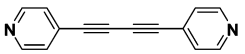	208	0.06	143	72	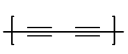	0.019
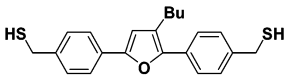	99.2	0.13	34.8	73	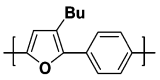	0.037
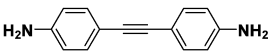	23.3	0.202	5.40	74	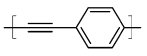	0.056
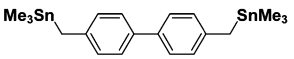	0.129	0.43	0.00213	25	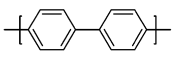	0.78 (*via* π channel)[75]
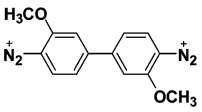	5.61	NA	0.00307	27	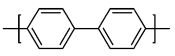	23.6 (*via* σ channel)[75]
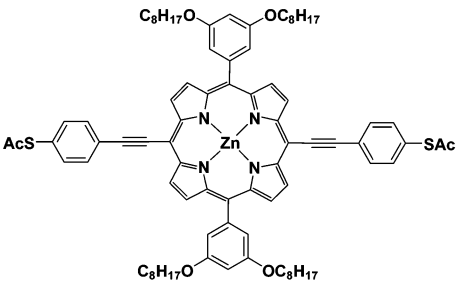	477	0.04	258	46	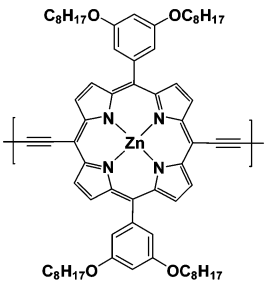	0.024
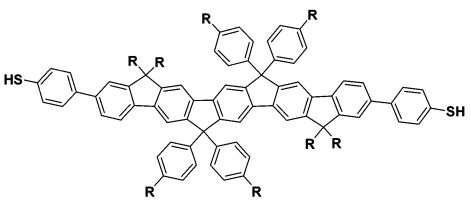	1315	0.206	15.9	76	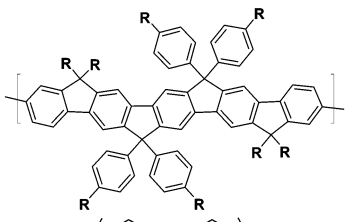	1.1
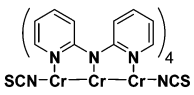	0.921	0.21	0.206	17	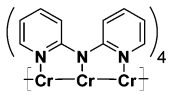	0.058
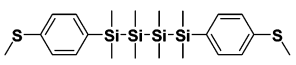	992	0.27	110	77	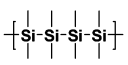	0.12

[a]Each of the cited literature reports carried out measurements of molecules with repeated units, and thus, the corresponding reference contains β values and $R_{n=0}$, except the biphenyls in which the contact resistance was employed from ref 24. [b]To estimate the resistance for the decoupled moieties, the measured MMM resistance (column 2) is divided by the contact resistance with the same headgroup−electrode combination. Note that these moieties have different lengths. [c]Note that the quality of the estimation deteriorates with reducing energy gaps of the molecular frontier orbitals or with reducing $|E_{FMO} - E_{Fermi}|$.

with N repeated units, and subsequently extract the effect of the contact to confer the conductance of the single molecular unit. As the mentioned previously, Green's function can express the amplitude of an electron propagating through a molecule. To outline the transmission from the left anchor group to the right, the integral term $(\mathbb{G}_{mol})_{l,r}$ is utilized from the element of the $\mathbb{G}_{mol}$ matrix. The $\mathbb{G}_{mol}$ matrix is derived from the tight-binding bridged model and the self-energy contributed from the electrodes (for details, see eqs S1−4 of the Supporting Information). The self-energy $\sum_{L(R)}$ describes the effects of the left (right) electrodes which impose shifts and broadening of the energy levels of the anchoring groups. For the limits of weak couplings (i.e., small $t_{L,l(r,R)}$ or $t_{L,l(r,R)} \ll |E_F - \varepsilon_m - \sum_{L(R)}|$, where E_F is the energy of the tunneling electron at the Fermi level, $t_{L,l(r,R)}$ stands for the resonance integral between the left (right) electrode and the left (right) anchoring group, ε_n is the on-site energy of site n, and $m = l$, r, and n), the Green's function of molecules with N repeated units, $(\mathbb{G}_{mol})_{l,r}$, can be expressed as follows

$$(\mathbb{G}_{mol})_{l,r} \propto \frac{1}{E_F - \varepsilon_N} \prod_{N-1}^{n=1} \frac{t_{n,n+1}}{E_F - \varepsilon_n} \quad for\ N \geq 2 \tag{1}$$

where $t_{n,n+1}$ is the resonance integral between nearest neighbor units (also termed as hopping integral in second quantization formalism). Note that eq 1 is consistent with that of the donor−bridge−acceptor model by Nitzan[78,79] and that $N \geq 2$ according to the product of sequences, $\prod_{n=1}^{N-1}$. For the limits of

dx.doi.org/10.1021/ja4088538 | J. Am. Chem. Soc. XXXX, XXX, XXX−XXX

weak coupling (i.e., $t_{n,n+1} \ll |E_F - \varepsilon_n|$), E_F lies within the HOMO−LUMO gap of the bridged molecule, corresponding to off-resonant tunneling.

For a homologous series, every unit presumably has the same ε_n and $t_{n,n+1}$, i.e., $\varepsilon_n = \varepsilon$ and $t_{n,n+1} = t$. Accordingly, the transmission function at the Fermi level $T(E_F)$ is obtained by incorporating Γ, the coupling function of the electrode with the anchoring group. Hence, eq 2 can be derived for the transmission, T_N (see eq S8 in the Supporting Information for details), that describes the transmission of the tunneling electron from the left (right) electrode passing through N units of the molecular backbone and then to the right (left) electrode.

$$T_N(E_F) = (\Gamma_L)_{l,l}(\Gamma_R)_{r,r}|(\mathbb{G}_{mol})_{l,r}|^2 = T_{contact}\left|\frac{t}{E_F - \varepsilon}\right|^{2N} \quad (2)$$

$$T_{contact} = \frac{(\Gamma_L)_{l,l}|t_{l,1}|^2}{|E_F - \varepsilon_l - (\sum_L)_{l,l}|^2}\frac{(\Gamma_R)_{r,r}|t_{N,r}|^2}{|E_F - \varepsilon_r - (\sum_R)_{r,r}|^2}\frac{1}{|t|^2} \quad (3)$$

Given that $G_{mol} \propto \exp(-\beta_n N)$ or $\exp(-\beta L)$, the attenuation parameter becomes

$$\beta_n(\text{per unit}) = 2\ln\left|\frac{E_F - \varepsilon}{t}\right| \quad \text{or}$$

$$\beta(\text{per Å}) = \frac{2N}{L}\ln\left|\frac{E_F - \varepsilon}{t}\right| \quad (4)$$

in which L is the length of the molecule (in Å). Equation 4 is also consistent with that of the donor−bridge−acceptor model by Nitzan.[78,79] Furthermore, the Green's function of molecules without repeated units, $(\mathbb{G}_{mol})_{l,r}$, can be expressed as follows

$$(\mathbb{G}_{mol})_{l,r} = \frac{t_{l,1}}{E_F - \varepsilon_l - \Sigma_L}\frac{t_{1,r}}{E_F - \varepsilon_r - \Sigma_R}\frac{1}{E_F - \varepsilon} \quad \text{for 1 unit} \quad (5)$$

Similarly, the transmission function of molecules without repeated units, T_1, can be expressed as follows

$$T_1(E_F) = (\Gamma_L)_{l,l}(\Gamma_R)_{r,r}|(\mathbb{G}_{mol})_{l,r}|^2 = \frac{(\Gamma_L)_{l,l}|t_{l,1}|^2}{|E_F - \varepsilon_l - (\sum_L)_{l,l}|^2}\cdot\frac{(\Gamma_R)_{r,r}|t_{1,r}|^2}{|E_F - \varepsilon_r - (\sum_R)_{r,r}|^2}\cdot\left|\frac{1}{E_F - \varepsilon}\right|^2 \quad \text{for 1 unit} \quad (6)$$

Note that $t_{l,1} = t_{1,r}$ because each repeated unit is identical so its coupling to anchoring group is the same. Since $G = G_0 T(E_F)$ gives the conductance of the MMM configuration, our proposed simplified approach decouples the contact component by dividing eq 6 with eq 3 and leads to the conductance of the molecular backbone, G_{unit}.

$$G_{unit} \equiv G_0\frac{T_1(E_F)}{T_{contact}} = G_0\left|\frac{t}{E_F - \varepsilon}\right|^2 \quad (7)$$

Equation 7 indicates that G_{unit} is independent from the self-energy contributed from the electrodes. Explicitly, G_{unit} is not sensitive to molecule-electrode contacts such as anchoring groups and the surface configurations of electrodes, consistent with our experiment observation. Therefore, even for those lack of repeated units (i.e., $N = 1$ case), G_{unit} can still be derived.

The numerator term, $|t|^2$, of eq 7 comes from the denominator $T_{contact}$ (see the last term of eq 3) which is extrapolated from a homologous series of molecules with repeated units (i.e., $N \geq 2$ cases). The presence of $|t|^2$ in eq 7 implies that, even for the $N = 1$ case, the conductance of the molecular backbone unit still inherits the resonance integral term as if there were repeated units. Note that our model is based on the condition of $\min|E_F - \varepsilon_m - \Sigma_{L(R)}| \gg \max|t_{m,m'}|$. Intriguingly, examples of $-(p\text{-}C_6H_4)-$ in Figure 7 and oligo(phenylene-ethylene) derivatives by Wandlowski et al.[68] (vide infra) manifest that the decoupled results obtained by using $G_{contact}$ of the aromatic backbone units are not significantly different from those with embedded $t_{n,n+1}$ of methylene units. The independence of $G_{contact}$ in different molecular systems deserves further theoretical exploration.

To summarize, we have the following conclusions in our analysis: (i) As $\min|E_F - \varepsilon_m - \Sigma_{L(R)}| \gg \max|t_{m,m'}|$, T_{unit} is independent from the self-energy contributed from the electrodes. Specifically, T_{unit} is not sensitive to molecule−electrode contacts. As a result, in the case that the types of two electrodes are the same (with the same Fermi level), we can define the conductance of the molecular backbone unit. (ii) In the case of the weak couplings between two sites as well as two electrodes with similar Fermi levels, the resistance of the molecular backbone unit should be similar. (iii) As $\min|E_F - \varepsilon_m - \Sigma_{L(R)}| \sim \max|t_{m,m'}|$, eq S4 for $(\mathbb{G}_{mol})_{l,r}$ becomes invalid. Hence, the transmission cannot be separated into the form, $T = T_{contact} \cdot (T_{unit})^N$. In this case, the conductance of the molecular backbone unit cannot be defined. (iv) Note that our conclusions are only valid in the case that the energies of HOMO or LUMO are far away from the Fermi levels, the weak couplings between neighboring units of the molecular backbone, the molecular backbones have no direct coupling to electrodes, and the anchoring groups have weak couplings to electrodes.

CONCLUSION

To assess the concept inherent in Landauer formulation that the conductance of tailored molecular segments can be estimated quantitatively, the electrical properties of alkanedinitriles are scrutinized to broaden the model systems and to make the model study more generalized. The molecular conductance measured using Pt electrodes for alkanedinitriles is found to be ca. 3-fold higher than those with Au and Pd. Simulated bond angles of ∠CNM by DFT calculations and Mayer bond order of N−M suggest that the superior conductance on Pt arises from stronger electronic coupling at CN−Pt contact. With this additional data set, variables at the contact increase to three headgroups (−SH, −NCS, and −CN) and three types of electrode materials (Au, Pd, and Pt). Cross examination on the conductance of molecular backbones is carried out by decoupling the contact resistance from the molecular conductance using the Landauer equation. The results show that the derived values for the same molecular moiety falls in a narrow conductance range, independent of the terminal headgroups and electrode materials. This approach is also applied to a range of conjugated moieties and organometallics. The weak coupling limits of the tight-binding model suggest that the decoupled resistance value for the molecular

dx.doi.org/10.1021/ja4088538 | J. Am. Chem. Soc. XXXX, XXX, XXX−XXX

framework is associated with its energy level and is independent of the headgroup−electrode interactions.

From a theoretical standpoint, we show that the resistance of the alkane backbones is not sensitive to molecule-electrode contacts under the conditions of weak couplings between two sites. However, it is still unknown why the resistance of the alkane backbones is not sensitive to the Fermi levels. This issue may originate from the fact that there are two conduction mechanisms, one for electron and one for hole conduction, and when one increases the other decreases. Alternatively there may be some yet unknown pinning mechanisms. The results present an interesting theoretical challenge and might be an interesting open theoretical problem.

■ ASSOCIATED CONTENT

Supporting Information

Conductance histograms and NEGF-DFT calculated conductance for alkanedinitriles; conductance of alkanedithiols and diisothiocyanates measured by Au, Pt, and Pt electrodes; derivation of molecular backbone conductance. This material is available free of charge via the Internet at http://pubs.acs.org.

■ AUTHOR INFORMATION

Corresponding Author

chhchen@ntu.edu.tw

Present Address

[†]Department of Chemistry, Princeton University, Princeton, New Jersey 08544, USA.

Author Contributions

[§]M.-J.H. and L.-Y.H. contributed equally to this work.

Notes

The authors declare no competing financial interest.

■ ACKNOWLEDGMENTS

The authors thank NTU (102R890911), NSC (Taiwan) (101-2628-M-002-012, 101-2113-M-002-001-MY2), and AOARD (FA2386-12-1 4006) for the financial support and thank the National Center for High-Performance Computing (Taiwan) for the computing time. Special thanks to Ms. Fang-Mei Chen for the preparation of the TOC graph.

■ REFERENCES

(1) Reed, M. A.; Zhou, C.; Muller, C. J.; Burgin, T. P.; Tour, J. M. *Science* **1997**, *278*, 252−254.

(2) Xu, B.; Tao, N. J. *Science* **2003**, *301*, 1221−1223.

(3) Haiss, W.; Nichols, R. J.; van Zalinge, H.; Higgins, S. J.; Bethell, D.; Schiffrin, D. J. *Phys. Chem. Chem. Phys.* **2004**, *6*, 4330−4337.

(4) Tao, N. *Nature Nanotechnol.* **2006**, *1*, 173−181.

(5) Morita, T.; Lindsay, S. *J. Am. Chem. Soc.* **2007**, *129*, 7262−7263.

(6) Venkataraman, L.; Klare, J. E.; Nuckolls, C.; Hybertsen, M. S.; Steigerwald, M. L. *Nature* **2006**, *442*, 904−907.

(7) Guo, X.; Jia, C. *Chem. Soc. Rev.* **2013**, *42*, 5642−5660.

(8) Aviram, A.; Ratner, M. A. *Chem. Phys. Lett.* **1974**, *29*, 277−283.

(9) Guo, X.; Small, J. P.; Klare, J. E.; Wang, Y.; Purewal, M. S.; Tam, I. W.; Hong, B. H.; Caldwell, R.; Huang, L.; O'Brien, S.; Yan, J.; Breslow, R.; Wind, S. J.; Hone, J.; Kim, P.; Nuckolls, C. *Science* **2006**, *311*, 356−359.

(10) Cao, Y.; Dong, S.; Liu, S.; He, L.; Gan, L.; Yu, X.; Steigerwald, M. L.; Wu, X.; Liu, Z.; Guo, X. *Angew. Chem. Int. Ed.* **2012**, *51*, 12228−12232.

(11) Tsutsui, M.; Shoji, K.; Taniguchi, M.; Kawai, T. *Nano Lett.* **2008**, *8*, 345−349.

(12) Wu, S.; Gonzalez, M. T.; Huber, R.; Grunder, S.; Mayor, M.; Schonenberger, C.; Calame, M. *Nature Nanotechnol.* **2008**, *3*, 569−574.

(13) Kiguchi, M.; Murakoshi, K. *J. Phys. Chem. C* **2008**, *112*, 8140−8143.

(14) Lortscher, E.; Ciszek, J. W.; Tour, J.; Riel, H. *Small* **2006**, *2*, 973−977.

(15) Kim, Y.; Hellmuth, T. J.; Burkle, M.; Pauly, F.; Scheer, E. *ACS Nano* **2011**, *5*, 4104−4111.

(16) Xu, B.; Xiao, X.; Tao, N. J. *J. Am. Chem. Soc.* **2003**, *125*, 16164−16165.

(17) Chen, I-W. P.; Fu, M.-D.; Tseng, W.-H.; Yu, J.-Y.; Wu, S.-H.; Ku, C.-J.; Chen, C.-h.; Peng, S.-M. *Angew. Chem. Int. Ed.* **2006**, *45*, 5814−5818.

(18) Leary, E.; Higgins, S. J.; van Zalinge, H.; Haiss, W.; Nichols, R. J. *Chem. Commun.* **2007**, 3939−3941.

(19) Li, C.; Pobelov, I.; Wandlowski, T.; Bagrets, A.; Arnold, A.; Evers, F. *J. Am. Chem. Soc.* **2008**, *130*, 318−326.

(20) Park, Y. S.; Whalley, A. C.; Kamenetska, M.; Steigerwald, M. L.; Hybertsen, M. S.; Nuckolls, C.; Venkataraman, L. *J. Am. Chem. Soc.* **2007**, *129*, 15768−15769.

(21) Frei, M.; Aradhya, S. V.; Hybertsen, M. S.; Venkataraman, L. *J. Am. Chem. Soc.* **2012**, *134*, 4003−4006.

(22) Yamada, R.; Kumazawa, H.; Noutoshi, T.; Tanaka, S.; Tada, H. *Nano Lett.* **2008**, *8*, 1237−1240.

(23) Chen, I-W. P.; Tseng, W.-H.; Gu, M.-W.; Su, L.-C.; Hsu, C.-H.; Chang, W.-H.; Chen, C.-h. *Angew. Chem. Int. Ed.* **2013**, *52*, 2449−2453.

(24) Cheng, Z. L.; Skouta, R.; Vazquez, H.; Widawsky, J. R.; Schneebeli, S.; Chen, W.; Hybertsen, M. S.; Breslow, R.; Venkataraman, L. *Nature Nanotechnol.* **2011**, *6*, 353−357.

(25) Chen, W. B.; Widawsky, J. R.; Vazquez, H.; Schneebeli, S. T.; Hybertsen, M. S.; Breslow, R.; Venkataraman, L. *J. Am. Chem. Soc.* **2011**, *133*, 17160−17163.

(26) Hong, W. J.; Li, H.; Liu, S. X.; Fu, Y. C.; Li, J. F.; Kaliginedi, V.; Decurtins, S.; Wandlowski, T. *J. Am. Chem. Soc.* **2012**, *134*, 19425−19431.

(27) Hines, T.; Díez-Pérez, I.; Nakamura, H.; Shimazaki, T.; Asai, Y.; Tao, N. *J. Am. Chem. Soc.* **2013**, *135*, 3319−3322.

(28) Chen, F.; Li, X.; Hihath, J.; Huang, Z.; Tao, N. *J. Am. Chem. Soc.* **2006**, *128*, 15874−15881.

(29) Li, X.; He, J.; Hihath, J.; Xu, B.; Lindsay, S. M.; Tao, N. *J. Am. Chem. Soc.* **2006**, *128*, 2135−2141.

(30) Fu, M.-D.; Chen, I-W. P.; Lu, H.-C.; Kuo, C.-T.; Tseng, W.-H.; Chen, C.-h. *J. Phys. Chem. C* **2007**, *111*, 11450−11455.

(31) Quek, S. Y.; Kamenetska, M.; Steigerwald, M. L.; Choi, H. J.; Louie, S. G.; Hybertsen, M. S.; Neaton, J. B.; Venkataraman, L. *Nature Nanotechnol.* **2009**, *4*, 230−234.

(32) Haiss, W.; Martin, S.; Leary, E.; van Zalinge, H.; Higgins, S. J.; Bouffier, L.; Nichols, R. J. *J. Phys. Chem. C* **2009**, *113*, 5823−5833.

(33) Kim, C. M.; Bechhoefer, J. *J. Chem. Phys.* **2013**, *138*, 014707.

(34) Kaun, C. C.; Seideman, T. *Phys. Rev. B* **2008**, *77*, 033414.

(35) Sheng, W.; Li, Z. Y.; Ning, Z. Y.; Zhang, Z. H.; Yang, Z. Q.; Guo, H. *J. Chem. Phys.* **2009**, *131*, 244714.

(36) Basch, H.; Cohen, R.; Ratner, M. A. *Nano Lett.* **2005**, *5*, 1668−1675.

(37) Jang, S.-Y.; Reddy, P.; Majumdar, A.; Segalman, R. A. *Nano Lett.* **2006**, *6*, 2362−2367.

(38) Ko, C.-H.; Huang, M.-J.; Fu, M.-D.; Chen, C.-h. *J. Am. Chem. Soc.* **2010**, *132*, 756−764.

(39) Kim, Y.; Song, H.; Strigl, F.; Pernau, H. F.; Lee, T.; Scheer, E. *Phys. Rev. Lett.* **2011**, *106*, 196804.

(40) Xiao, X.; Xu, B.; Tao, N. J. *Nano Lett.* **2004**, *4*, 267−271.

(41) Ashcroft, N. W.; Mermin, N. D. *Solid State Physics*: Saunders College: Philadelphia, 1976.

(42) Gorelsky, S. I. *AOMix: Program for Molecular Orbital Analysis*, University of Ottawa: Ottawa, 2009, http://www.sg-chem.net/.

(43) Gorelsky, S. I.; Lever, A. B. P. *J. Organomet. Chem.* **2001**, *635*, 187−196.

(44) Hong, W. J.; Manrique, D. Z.; Moreno-Garcia, P.; Gulcur, M.; Mishchenko, A.; Lambert, C. J.; Bryce, M. R.; Wandlowski, T. *J. Am. Chem. Soc.* **2012**, *134*, 2292−2304.
(45) Kim, B.; Beebe, J. M.; Jun, Y.; Zhu, X. Y.; Frisbie, C. D. *J. Am. Chem. Soc.* **2006**, *128*, 4970−4971.
(46) Sedghi, G.; Sawada, K.; Esdaile, L. J.; Hoffmann, M.; Anderson, H. L.; Bethell, D.; Haiss, W.; Higgins, S. J.; Nichols, R. J. *J. Am. Chem. Soc.* **2008**, *130*, 8582−8583.
(47) Li, Z. H.; Park, T. H.; Rawson, J.; Therien, M. J.; Borguet, E. *Nano Lett.* **2012**, *12*, 2722−2727.
(48) Cui, X. D.; Primak, A.; Zarate, X.; Tomfohr, J.; Sankey, O. F.; Moore, A. L.; Moore, T. A.; Gust, D.; Nagahara, L. A.; Lindsay, S. M. *J. Phys. Chem. B* **2002**, *106*, 8609−8614.
(49) Seminario, J. M.; De la Cruz, C. E.; Derosa, P. A. *J. Am. Chem. Soc.* **2001**, *123*, 5616−5617.
(50) Engelkes, V. B.; Beebe, J. M.; Frisbie, C. D. *J. Am. Chem. Soc.* **2004**, *126*, 14287−14296.
(51) Beebe, J. M.; Kim, B.; Frisbie, C. D.; Kushmerick, J. G. *ACS Nano* **2008**, *2*, 827−832.
(52) Dulic, D.; Van der Molen, S. J.; Kudernac, T.; Jonkman, H. T.; de Jong, J. J. D.; Bowden, T. N.; van Esch, J.; Feringa, B. L.; van Wees, B. J. *Phys. Rev. Lett.* **2003**, *91*, 207402.
(53) Whalley, A. C.; Steigerwald, M. L.; Guo, X.; Nuckolls, C. *J. Am. Chem. Soc.* **2007**, *129*, 12590−12591.
(54) Jia, C.; Wang, J.; Yao, C.; Cao, Y.; Zhong, Y.; Liu, Z.; Liu, Z.; Guo, X. *Angew. Chem. Int. Ed.* **2013**, *52*, 8666−8670.
(55) Less, K. J.; Wilson, E. G. *J. Phys. C: Solid State Phys.* **1973**, *6*, 3110−3121.
(56) Boulas, C.; Davidovits, J. V.; Rondelez, F.; Vuillaume, D. *Phys. Rev. Lett.* **1996**, *76*, 4797−4800.
(57) Papaconstantopoulos, D. A. *Handbook of the Band Structure of Elemental Solids*; Springer: New York, 1986; pp 157−160 and 195−202.
(58) Kaun, C. C.; Guo, H. *Nano Lett.* **2003**, *3*, 1521−1525.
(59) Crljen, Z.; Grigoriev, A.; Wendin, G.; Stokbro, K. *Phys. Rev. B* **2005**, *71*, 165316.
(60) Zhou, Y. X.; Jiang, F.; Chen, H.; Note, R.; Mizuseki, H.; Kawazoe, Y. *J. Chem. Phys.* **2008**, *128*, 044704.
(61) Malen, J. A.; Doak, P.; Baheti, K.; Tilley, T. D.; Segalman, R. A.; Majumdar, A. *Nano Lett.* **2009**, *9*, 1164−1169.
(62) Kamenetska, M.; Quek, S. Y.; Whalley, A. C.; Steigerwald, M. L.; Choi, H. J.; Louie, S. G.; Nuckolls, C.; Hybertsen, M. S.; Neaton, J. B.; Venkataraman, L. *J. Am. Chem. Soc.* **2010**, *132*, 6817−6821.
(63) Chen, F.; Tao, N. J. *Acc. Chem. Res.* **2009**, *42*, 429−438.
(64) Song, H.; Kim, Y.; Jang, Y. H.; Jeong, H.; Reed, M. A.; Lee, T. *Nature* **2009**, *462*, 1039−1043.
(65) Kim, Y.; Pietsch, T.; Erbe, A.; Belzig, W.; Scheer, E. *Nano Lett.* **2011**, *11*, 3734−3738.
(66) Bruot, C.; Hihath, J.; Tao, N. J. *Nature Nanotechnol.* **2012**, *7*, 35−40.
(67) Diez-Perez, I.; Hihath, J.; Lee, Y.; Yu, L. P.; Adamska, L.; Kozhushner, M. A.; Oleynik, I. I.; Tao, N. J. *Nature Chem.* **2009**, *1*, 635−641.
(68) Kaliginedi, V.; Moreno-Garcia, P.; Valkenier, H.; Hong, W. J.; Garcia-Suarez, V. M.; Buiter, P.; Otten, J. L. H.; Hummelen, J. C.; Lambert, C. J.; Wandlowski, T. *J. Am. Chem. Soc.* **2012**, *134*, 5262−5275.
(69) The Au−S contact resistance of 1,4-phenyls is obtained from the conductance of benzenedithiol (0.011 G_0)[40] and tetraphenyldithiol (4.5×10^{-5} G_0).[67]
(70) Ma, G. H.; Shen, X.; Sun, L. L.; Zhang, R. X.; Wei, P.; Sanvito, S.; Hou, S. M. *Nanotechnology* **2010**, *21*, 495202.
(71) Simmons, J. G. *J. Appl. Phys.* **1963**, *34*, 1793−1803.
(72) Wang, C. S.; Batsanov, A. S.; Bryce, M. R.; Martin, S.; Nichols, R. J.; Higgins, S. J.; Garcia-Suarez, V. M.; Lambert, C. J. *J. Am. Chem. Soc.* **2009**, *131*, 15647−15654.
(73) Chen, I-W. P.; Fu, M.-D.; Tseng, W.-H.; Chen, C.-h.; Chou, C.-M.; Luh, T.-Y. *Chem. Commun.* **2007**, 3074−3076.
(74) Lu, Q.; Liu, K.; Zhang, H. M.; Du, Z. B.; Wang, X. H.; Wang, F. S. *ACS Nano* **2009**, *3*, 3861−3868.
(75) Two sets of estimated resistance are suggested for −(p-C_6H_4)− and biphenyl moieties, ascribed to the disparity in the π- or σ-channels for charge transport.[24,27] Based on the calculations for the Au−(p-C_6H_4)−Au system by Venkataraman et al., the energy level of the σ-bonding orbitals is 0.9 eV, lower than that of the π-bonding orbitals (0.83 eV).[24] This finding indicates that the energy barrier of the σ-channel pathway is larger than that of the π channel; viz., the former has a larger $|E_F - \varepsilon|$ (eq 4). Hence, the σ channel offers a less conductive pathway than those via the π channel. Note that for the Au−(p-C_6H_4)−Au junction, the dominant pathway is the σ-channel with the transmission of 24% against 1.6% of the π-channel.[24] The covalent aromatic carbon-gold bonds (refs 24 and 27) are the only two examples that the charge transport is not dominated by the frontier orbitals, i.e., the π-channel pathway.
(76) Hines, T.; Diez-Perez, I.; Hihath, J.; Liu, H. M.; Wang, Z. S.; Zhao, J. W.; Zhou, G.; Muellen, K.; Tao, N. J. *J. Am. Chem. Soc.* **2010**, *132*, 11658−11664.
(77) Klausen, R. S.; Widawsky, J. R.; Steigerwald, M. L.; Venkataraman, L.; Nuckolls, C. *J. Am. Chem. Soc.* **2012**, *134*, 4541−4544.
(78) Nitzan, A. *J. Phys. Chem. A* **2001**, *105*, 2677−2679.
(79) Nitzan, A. *Annu. Rev. Phys. Chem.* **2001**, *52*, 681−750.